Experimental Verification of Simulated Blocked Forces in Wastewater System using the Empirical Model of Water-Flow Excitation

Yohko Aoki[1], Sven Öhler[1], Bernd Kaltbeitzel[1]

[1]*Fraunhofer Institute for Building Physics IBP, Department Acoustics, Stuttgart, Germany*

This paper is a revised version of the authors' submitted manuscript that was peer-reviewed by at least two anonymous reviewers.

Abstract

Structure-borne sound generated by wastewater pipe systems often dominates noise emissions from sanitary installations in buildings. This noise is mainly caused by turbulent annular flow and by water impacts on inlets, tees, and bends. The water excitation, and thus the resulting structural response, is treated as a stochastic process and described by its power spectral density (PSD). A suitable mathematical model of PSD for the individual excitation sub-sources of the water-induced loads on a wastewater pipe is developed in a systematic, stepwise manner by combining experimental data with a numerical model. Both experimental and numerical configurations comply with EN 14366-1:2023 [1], with the vibration response quantified by the blocked forces at the wall fixing points. The turbulent annular film flow along the inner pipe wall is represented by a PSD function that appears linear in double logarithmic scale, while the water impact on the basement bend is modelled by a Gaussian-shaped function. The PSD parameters are identified using the least squares method to minimize the difference between measured and simulated blocked forces. The quantified excitation terms are incorporated into the numerical models, and the simulated blocked forces are compared with the measurements. The overall agreement is satisfactory and supports the applicability of the proposed method for predicting structure-borne noise from wastewater systems.

Keywords : *drain pipe, structure-borne noise, EN 14366-1, flow-induced excitation, FEM*

Corresponding author: yohko.aoki@ ibp.fraunhofer.de

1. Introduction

Wastewater noise can affect adjacent rooms in buildings [1]. In vertical wastewater pipes, water forms a thin annular film with entrained air bubbles along the inner wall, while air flows through the pipe core [2]. This annular flow causes unsteady wall-pressure fluctuations; bends, inlets, and tees add impact excitation [3]. These excitations induce pipe vibrations that are transmitted through clamps into the building structure and radiated as airborne sound.

Knowledge of the magnitude and frequency spectrum of flow-induced forces is essential for acoustically optimized drainpipes. However, direct simulation of two-phase gas-liquid flow remains computationally demanding [4], and stochastic water excitation is difficult to determine experimentally. Although excitation at bends and discontinuities has been studied [5], no comprehensive analytical model for wastewater excitation is available.

By contrast, the pipe vibration response can be measured reliably [6]. Indirect methods therefore reconstruct the unknown water excitation from measured output by inverting a mechanical model. This is challenging because inverse methods may amplify numerical and experimental uncertainties, leading to inaccurate load estimates [7].

In our previous study [3], the inverse approach was applied to estimate the shaker induced point force from measured blocked forces and a validated FE model of the drainpipe system. The results showed that the approach is useful, provided that the excitation input is represented appropriately.

This study aims to estimate water-induced excitation loads in a drainpipe system. It introduces an analytical stochastic-load model whose PSD depends on frequency and volume flow rate. The frequency dependence is derived empirically from measurements (Section 3), and the flow-rate dependence is identified numerically (Section 4). Simulated and measured blocked forces are then compared to assess the proposed approach.

2. Physical arrangement

This section summarizes the physical configuration of the investigated wastewater system and its numerical model.

2.1 Experiments

Structure-borne and airborne noise were measured according to EN 14366-1 [1]. Figure 1 shows the standard wastewater test setup at Fraunhofer IBP in Stuttgart. The pipe has an outer diameter of 110 mm and a wall thickness of 3.2 mm and extends over four floors. According to EN 14366-1 [1], the rooms above the basement bend are the test rooms; these correspond to “UG rear” and “UG front” in the present facility. This paper therefore evaluates only results from the test floor. The pipes are fixed to the installation wall with steel clamps with rubber inlays at about 2.5 m and 0.5 m above each floor. The clamps are anchored with M10 bolts and plastic dowels, and the pipe response is assessed by the blocked forces [1] at these two contact points.

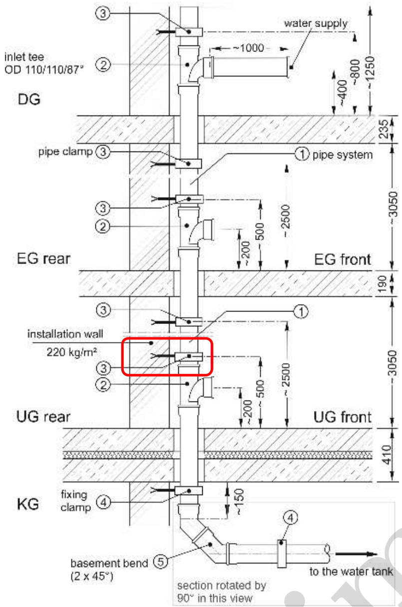

Figure 1. Test facility with the standard wastewater system set-up at Fraunhofer IBP, Stuttgart for measurements according to EN 14366-1 [1]. KG: basement; UG: test floor; EG: ground floor; DG: top floor. Red box: lower clamp on the test floor.

The excitation sources of the standard pipe setup are separated into four components: annular water flow on the pipe wall, impact force at the water inlet, water impact at the tees on the ground floor and underground floor, and water impact at the basement bend. Previous work [3] showed that the response on the test floor is dominated by annular flow and bend impact, while inlet and tee contributions are small. Therefore, this paper focuses on annular flow and bend impact.
To separate each excitation source, the pipe setup was modified from the standard configuration (Figure 1) to:

STR: Fully straight pipe with total length of 8.34 m, equipped with a customized impact-free inlet.

NoT: The standard configuration without tees (otherwise identical to standard; with bend).

The impact-free inlet was designed at IBP to minimize hydraulic disturbances at the water supply [3]. In the STR configuration, the dominant excitation is therefore turbulent annular flow, while inlet impacts are negligible. In the NoT configuration, the standard inlet was used because the impact-free inlet had an air-supply limitation. Although this adds inlet excitation, its influence decreases with distance and is negligible on the test floor. Thus, NoT remains suitable for isolating the effect of the basement bend on the blocked force at the test floor.
According to the standard [1], measurements cover 1/3-octave bands from 50 Hz to 5 kHz. The present analysis is limited to 1 kHz because the investigated systems are dominated by components below 1 kHz in both measured sound pressure level and the corresponding single-number quantity, even after A-weighting.

2.2 FE Simulation with COMSOL

In addition to the experiments, a finite element (FE) model of the pipe system [3] in COMSOL Multiphysics was developed to predict the blocked forces at the clamp positions. This model was validated in our previous study [3] using shaker measurements with a known deterministic input force.
The straight-pipe configuration (STR) is modeled as a circular cylindrical shell with six pipe clamps and free boundary conditions at both ends. The impact-free inlet is omitted because it has no direct mechanical contact with the pipe. For the No-Tee configuration (NoT), the 45-degree basement bend with a centerline length of 0.25 m and a 0.5 m horizontal pipe segment are added (⑤ in Figure 1). The horizontal pipe is truncated at the additional clamp position (clamp ④ in ‘KG’ in Figure 1), where all translational and rotational degrees of freedom are constrained.
The same material properties and wall thickness are assigned to the straight, bend, and horizontal pipe sections.
Table 1 summarizes the material parameters of the pipe system as well as the hydrodynamic mass, which is the equivalent mass of fluid vibrating together with the structure [10].

Table 1. Material parameters of the drainpipe systems used in the FE model.

parameter		pipe	clamp
E-module [GPa]		3.92	203
poisson’s ratio [-]		0.3	0.3
loss factor [-]		0.055	0.005
density [kg/m^3]	flowrate	1850	7850
	1.0 l/s	+ 74	--
	1.5 l/s	+ 98	--
	2.0 l/s	+ 122	--
	3.0 l/s	+ 177	--

The hydrodynamic added mass was estimated using the eigenfrequencies of the water loaded pipe system, f_r, measured by operational modal analysis [9].

$$\mu_h = \mu_p \left[\left(\frac{f_{air}}{f_r} \right)^2 - 1 \right] \quad (1)$$

where f_{air} is the resonant frequency of the dry pipe, i.e. a pipe without the hydrodynamic added mass of the water, and μ_p and μ_h respectively denote the line density of the pipe and the hydrodynamic added mass.

The flow-induced loading in the pipe is considered an ergodic and stationary random process. Therefore, the *Random Vibration* interface in COMSOL is used, in which the excitation is given by its power spectral density (PSD). The random vibration analysis is performed using modal superposition: all eigenmodes with eigenfrequencies up to approximately 1 kHz are included. The blocked forces are simulated in the range from 20 Hz to 1 kHz with a frequency resolution of 1 Hz.

In the FE model, both the turbulent annular flow and the water impact at the bend are modeled as fluctuating wall pressures acting on the pipe surface. The corresponding PSDs are therefore expressed in units of mean-square pressure per unit bandwidth, $(N/m^2)^2/Hz$. The water load due to the annular flow is applied in the x and y direction on the wall of the vertical pipe, whereas the water impact at the basement bend is applied in the vertical direction (along gravity, the z direction) on the lower inclined surface of the bend (see Figure 2). The two stochastic excitation fields are assumed to be mutually uncorrelated.

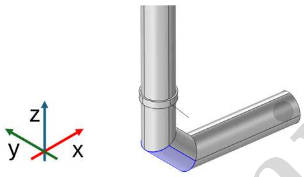

Figure 2. Magnified view around the basement bend of the pipe system in FE model, highlighting the excitation region (blue).

In general, the PSD of flow excitation depends on frequency, position, and volume flow rate. Here, spatial dependence is neglected. Bend impact is applied with uniform amplitude over the corresponding pipe surface. For annular flow, the flow is assumed to be fully developed and approximately uniform along the vertical pipe section after a short inlet distance. Although simplified, this assumption provides a practical basis for estimating steady-flow excitation.

3. Empirical Models of Excitation

In this section, an empirical model for the water-induced excitation is developed. First, the experimental results are analyzed to characterize the excitation. Then, based on these results, mathematical expressions are derived for the PSD of each excitation contribution.

3.1 Annular Film Flow

When the flow is turbulent, the small random fluctuations in flow velocity and in the associated pressure field can excite the pipe structure. The pressure fluctuations have a wide frequency spectrum [11]. The Reynolds number of the thin water film along the pipe wall is defined as [11]:

$$Re = \frac{\rho U_m t_{film}}{\mu} \quad (2)$$

where U_m is the mean flow velocity and t_{film} is the characteristic length, i.e. the film thickness [3]. At 20°C, water density and dynamic viscosity are taken as $\rho = 1000\ \mathrm{kg/m^3}$ and $\mu = 1.0 \times 10^{-3}\ \mathrm{Pa \cdot s}$. Table 2 shows Reynolds numbers between 3000 and 9000, well above the transition threshold for thin film flow ($Re \sim 1600$) [11]. The film flow is therefore treated as fully turbulent.

Table 2. Parameters of annular film flow in the pipe for four different volume flow rates.

parameter	1.0 l/s	1.5 l/s	2.0 l/s	3.0 l/s
U_m [m/s]	3.89	4.62	5.12	5.50
t_{film} [mm]	0.8	1.1	1.3	1.8
Reynolds number	3067	4600	6133	9200

Figure 3 shows blocked forces derived from STR measurements at the lower clamp on the test floor for volume flow rates from 1.0 l/s to 3.0 l/s. The blocked force was obtained indirectly from the installed power and receiver mobility [1] and is expressed in dB re 10^{-6} N. The 1/24-octave spectra have very similar shapes: increasing the flow rate mainly shifts the level upward by about 1–3 dB, while the spectral shape remains nearly unchanged. Thus, the PSD can be represented by a common frequency-dependent shape function multiplied by a flow-rate-dependent scaling factor.

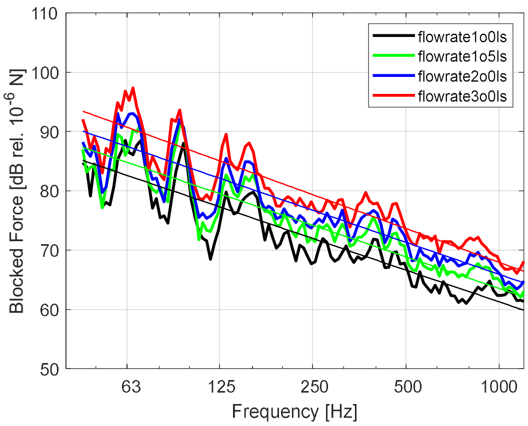

Figure 3. Measured blocked force of straight pipe (STR) on the lower clamp on the test floor for various volume flow rates (solid lines), and its guidelines (thin lines).

In Fig. 3, the blocked force decreases monotonically as frequency rises with only minor oscillations. These oscillations are more pronounced at low frequencies and therefore are presumably linked to structural resonances. Up to 1 kHz, the response decreases approximately linearly on a double-logarithmic scale, as indicated by the thin guidelines added to Figure 3. Accordingly, the PSD of the annular turbulent flow is approximated by

$$PSD_{flow}(f,Q) = C_{flow}(Q)\, f^N \qquad (3)$$

which appears as a straight line on a double-logarithmic scale.
In the formula, N is the exponent and $C_{flow}(Q)$ is the scaling factor that depends on the volume flow rate Q in m^3/s. These parameters are determined numerically in Section 4.

3.2 Water Impact on the Basement Bend

Figure 4 shows the difference between the blocked force levels derived from the NoT and STR measurements at the lower clamp on the test floor, shown in 1/24-octave bands.

$$\Delta L_{Fb} = L_{Fb,NoT} - L_{Fb,STR} \qquad (4)$$

Again, the four spectra show almost identical shapes, but the overall amplitude variation with volume flow rate is smaller than that observed for STR in Fig. 3. These four spectra are characterized by a sharp peak centered around 70 Hz. For the highest volume flow rate of 3.0 l/s, the peak amplitude associated with water impact on the bend reaches nearly 18 dB. Additionally, a broader maximum appears between 250 Hz and 500 Hz, with a lower amplitude of around 8 dB.

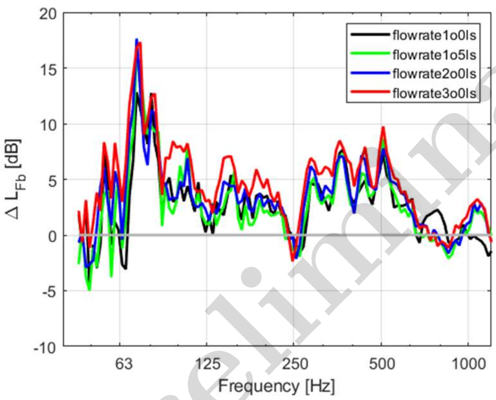

Figure 4. Difference between the blocked force levels derived from the NoT and STR measurements at the lower clamp on the test floor for various volume flow rates.

Since the peak at 70 Hz is more prominent, only this contribution is represented in the empirical PSD model for the water-impact excitation on the basement bend. In this log-frequency plot, the sharp peak around 70 Hz can be well approximated by a Gaussian function:

$$PSD_{bend}(f,Q) = C_{bend}(Q)\exp\left(-\frac{b}{2}(\log_{10}(f/f_c))^2\right) \qquad (5)$$

where f_c is the peak frequency and b controls the peak width. Unlike the standard deviation of a Gaussian in linear frequency, this parameter has no direct bandwidth interpretation on a double-logarithmic scale. C_{bend} is the volume-flow-rate-dependent scaling factor for bend impact.

4. Simulation Results

The empirical PSD formulas with initial parameters are applied to the FE models as input loads. The simulated blocked forces $L_{Fb,sim}$ are compared with blocked forces derived from measurements $L_{Fb,exp}$ to identify the PSD parameters. The least squares method is used at the lower clamp on the test floor, indicated by the red box in Figure 1:

$$H(\omega) = \left|L_{Fb,exp} - L_{Fb,sim}\right|^2 \qquad (6)$$

The lowest clamp is selected for two reasons: (i) the annular flow has reached the constant mean velocity far above this location [3], so the blocked force at this clamp is only weakly affected by flow acceleration and variations in hydrodynamic mass; and (ii) the basement bend has its strongest influence on the response at this lower clamp, while its effect diminishes at higher clamps because each clamp partially segments the pipe. While 1/24-octave bands were used in the previous section, blocked forces are now evaluated in 1/3-octave bands, consistent with the standard [1]. Unless stated, a volume flow rate of 2.0 l/s is shown in the comparisons between simulations and measurements, as this operating condition exhibits the highest repeatability and the strongest connection to real-life situations (flushing a toilet), while the PSD parameters are estimated for all volume flow rates.

4.1 Turbulent Flow

Figure 5 compares the simulated and measured blocked force of a straight pipe.

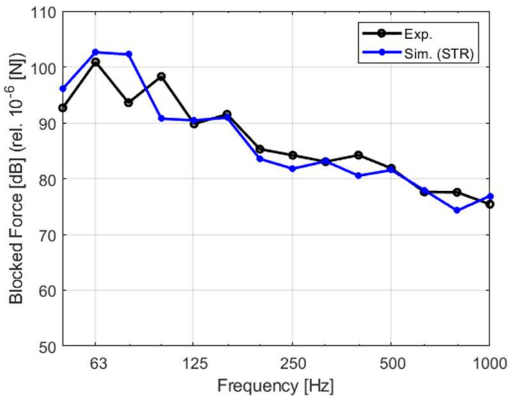

Figure 5. Comparison of measured (black) and simulated (blue) blocked force of the straight pipe (STR) at the lower clamp on the test floor for a volume flow rate of 2.0 l/s.

Overall, the simulated spectra follow the measurements reasonably well. At low frequencies, discrepancies of up to about 5 dB occur, mainly due to small shifts in the eigenfrequencies of the lowest modes between the numerical model and the test rig.
The optimized parameters of the PSD function in Eq. (3) are summarized in Table 3. For each volume flow rate, the parameters were optimized simultaneously using a local optimizer. The exponent

N was constrained to $-1 \leq N \leq 1$, while no bounds were applied to the PSD amplitude parameters. As shown in Table 3, the fitted frequency exponent is zero for all flow cases, i.e. the PSD is nearly frequency independent, which is equivalent to white noise excitation within the investigated frequency range. On the other hand, the amplitude of the PSD increases with the volume flow rate. The estimated PSD amplitude is well represented by a second-order polynomial of the volume flow rate, Q:

$$PSD_{flow}(Q) = a_{flow} Q^2 \quad (7)$$

where the constant $a_{flow} = 228$.

Table 3. Parameters of PSD function of the annular flow and the impact on the basement bend.

parameter	1.0 l/s	1.5 l/s	2.0 l/s	3.0 l/s
$C_{flow}(Q)$ 10^{-3}	0.35	0.68	1.02	1.95
exponent, N	0	0	0	0
$C_{bend}(Q)$	40.0	100.0	200.0	631
f_c [Hz]	76	76	76	76
width, b [--]	180	180	180	180

4.2 Water Impact on the Basement Bend

As a second step, the water impact on the basement bend is added to the FE model with the bend. The turbulent-flow excitation identified in Section 4.1 is applied along the straight segment of the pipe, while an additional local excitation term representing the water impact on the basement bend is applied at the corresponding elbow element (see Figure 2).

Table 3 summarizes the optimized parameters of the empirical PSD model for the water impact on the bend shown in Eq. (5). The peak frequency and width are nearly constant for all volume flow rates. The amplitude of the bend excitation is also approximated by a quadratic function of the volume flow rate, Q:

$$PSD_{bend}(f, Q) = a_{bend} Q^2 \exp\left(-\frac{b}{2}(\log_{10}(f/f_c))^2\right) \quad (8)$$

where $a_{bend} = 6.3 \times 10^7$.

Figure 6 compares simulated and measured blocked forces at the clamp.

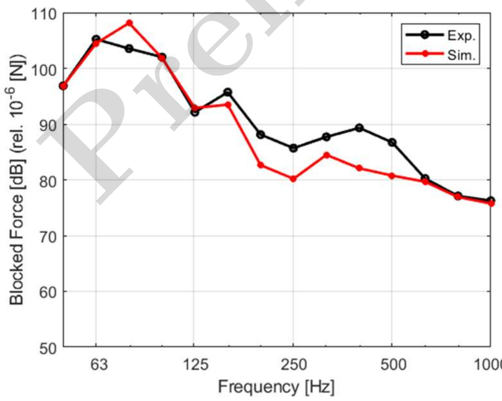

Figure 6. Comparison of measured (black) and simulated (red) blocked force of the No-Tee pipe (NoT) at the lower clamp on the test floor for a volume flow rate of 2.0 l/s.

The simulation captures the pronounced bend-impact peak around 70 Hz well. In contrast, agreement deteriorates between 250 Hz and 500 Hz. As shown in Figure 4, the bend produces both the sharp 70 Hz peak and a broadband increase in this mid-frequency range, whereas the present PSD model includes only the 70 Hz peak. Consequently, simulated levels are too low in the mid band. The physical origin of this broadband increase is unclear; possible causes include excitation from the horizontal basement pipe or additional discrete impact components. Nevertheless, the 70 Hz peak dominates the radiated sound and is the main feature to capture.

4.3 Estimated PSD functions

Figure 7 compares the PSD of the turbulent annular flow with that of the water impact at the basement bend for different volume flow rates. The PSD is shown in dB, referenced to 10^{-12} $(\mathrm{N/m^2})^2/\mathrm{Hz}$.

The previous experimental study [3] indicated that turbulent annular flow dominates the response at higher frequencies, while flow-turning elements have a pronounced influence in the low-frequency range. The identified PSDs are consistent with these observations.

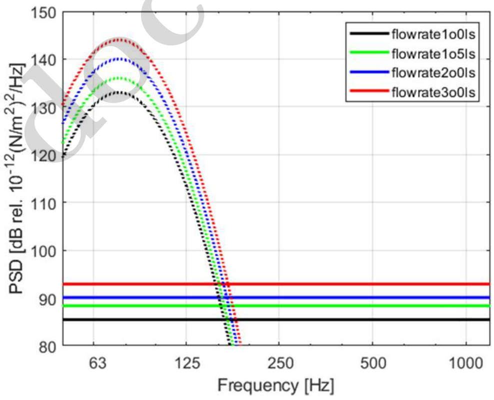

Figure 7. Estimated PSD of the annular flow (solid straight lines) and water impact at the bend (dotted curves) for volume flow rates of 1.0 l/s, 1.5 l/s, 2.0 l/s, and 3.0 l/s.

At the peak, the water impact PSD is more than 50 dB higher than the PSD of the annular flow. This difference is much larger than the maximum effect of the bend on the blocked forces shown in Figure 4, which was about 18 dB. The main reason is the direction of the excitation. The water impact is applied in the vertical direction on the 45-degree inclined surface of the bend, while the blocked forces are evaluated along the y-axis at the clamps (Figure 2). As a result, the structural transfer paths from the two excitation sources to the measured forces differ significantly.

5. Conclusions

This paper presented an empirical analytical model of the water-flow-induced excitation acting on a wastewater drainpipe. Among four potential

excitation sources, two dominant sources on the test floor, i.e. turbulent flow and water impact on the bend, were discussed in this paper.
The stochastic water-induced loads were modeled by combining blocked-force measurements with an FE model of the pipe system. Simple PSD functions were proposed for each excitation source: turbulent flow was initially represented by a linear function in double-logarithmic scale, and bend excitation by a Gaussian function. These PSDs were applied to the FE model and their parameters were identified by minimizing the difference between measured and simulated blocked forces. The turbulent-film-flow PSD was found to be nearly frequency independent up to 1 kHz, corresponding to white-noise excitation. The bend impact was well captured at low frequency by a Gaussian peak around 70 Hz, although agreement deteriorated in the mid-frequency range. In both cases, PSD amplitude was described by a second-order polynomial of volume flow rate.
The optimized PSDs were validated against measured blocked forces. For the straight pipe, deviations were generally within about 5 dB. With the bend included, the 70 Hz peak was reproduced well, while deviations in the mid-frequency range reached about 8 dB. Considering that repeated measurements after disassembly and reinstallation can vary by ±3 dB, the proposed excitation model provides a practical and sufficiently accurate basis for structure-borne simulations of wastewater pipes under the present modeling assumptions.
In future work, the excitation at the inlet should also be modelled, since the floor directly beneath the inlet is dominated by inlet-induced noise. Additionally, the proposed excitation model in this paper can be further extended and refined to reduce discrepancies between measurements and simulations. In particular, additional excitation terms from the bend or horizontal pipe section should be included to reduce the broadband discrepancy around 250–500 Hz.
Moreover, the frequency range should be extended up to 5 kHz to predict the sound pressure level in the receiving room using PreNoise [12]. This IBP-developed Web-based prediction tool can estimate structure-borne noise in buildings, based on EN 12354-5:2023 [8]. Extension of the frequency range can be achieved by complementing the existing 3D-cylindrical FE model with a simplified, beam-type representation of the pipe at higher frequencies.
Finally, parametric studies of material and geometric pipe properties will be carried out to optimize acoustic performance while minimizing material use. Because water flow is mainly governed by internal geometry and wall-friction characteristics, while its coupling to pipe vibration is comparatively weak, the excitation model is expected to remain applicable to pipes with similar internal properties, including systems made from biopolymers or recycled polymers.

6. Acknowledgments

We acknowledge financial support from The Federal Institute for Research on Building, Urban Affairs and Spatial Development (BBSR) Germany under grant number 10.08.18.7-24.60. We also extend our appreciation to Gebr. Ostendorf Kunststoffe GmbH, REHAU Industries SE & Co. KG, Orbia Building & Infrastructure (Wavin) and Wienerberger AG.

References

[1] EN 14366-1:2023, Laboratory measurement of airborne and structure-borne sound from service equipment – Part 1: Application rules for waste water installations, 2023.

[2] C. Monette, M. J. Pettigrew: "Fluidelastic instability of flexible tubes subjected to two-phase internal flow", *Journal of Fluids and Structures*, Vol. 19, Issue 7, pp. 943-956, 2004.

[3] Y. Aoki, S. Öhler, and B. Kaltbeitzel: "Preparatory Work Toward Experimental Estimation of Water Excitation Terms in Wastewater Systems", *Forum Acusticum* 2025 (Malaga, Spain), 2025.

[4] B. Song, C. Plana, et al.: "Phase-field simulation of core-annular pipe flow", *Int. J. of Multiphase Flow*, Vol. 117, pp. 14-24, 2019.

[5] J. L. Riverin, E. de Langre, M. J. Pettigrew: "Fluctuating forces caused by internal two-phase flow on bends and tees", *J. of Sound and Vibration* 298 (4-5), pp. 1088–1098, 2006.

[6] B. Kaltbeitzel, S. Öhler: "Latest results on the characterization of wastewater pipes according to the draft EN 14366-1", in *Proc. of Euronoise* 2021 (Madeira, Portugal), 2021.

[7] J. Sanchez, H. Benaroya: "Review of force reconstruction techniques", *J. of Sound and Vibration*, Vol. 333, Issue 14, 2999-3018, 2014.

[8] EN 12354-5:2023, Building acoustics - Estimation of acoustic performance of buildings from the performance of elements - Part 5: Sound levels due to service equipment, 2023.

[9] A. Filand, "*Numerische Analyse der Schwingungen eines Abwasserrohrs unter instationärer Fluidlast*", Master thesis, University of Stuttgart, 2022.

[10] M. P. Paidoussis, "*Fluid-Structure Interactions, Vol. 2: Slender Structures and Axial Flow*", 2nd edn., 2016.

[11] F. M. White, "Fluid mechanics", 7th edn., New York, NY: McGraw-Hill, 2011.

[12] PreNoise, https://prenoise.app/, accessed on 29.06.2026.